

TOPOLOGICAL OPTIMIZATION OF PIEZOELECTRIC ENERGY HARVESTING DEVICES FOR IMPROVED ELECTROMECHANICAL EFFICIENCY AND FREQUENCY RANGE

T. C. de Godoy¹, M. A. Trindade¹, J.-F. Deü²

¹ Department of Mechanical Engineering, São Carlos School of Engineering, University of São Paulo, São Carlos-SP, Brazil (tatiane.godoy@yahoo.com.br)

² Structural Mechanics and Coupled Systems Laboratory, Conservatoire National des Arts et Métiers, Paris, France

Abstract. *The development of energy harvesting devices with piezoelectric transducers has been widely studied in the last decade. Most of previous studies considered a resonant cantilever beam with an attached tip mass and focused on the proper modeling of the cantilever device, design and optimization of electric harvesting circuit and nonlinear amplification of resonant vibration amplitude. However, few studies focused on the optimization of the piezoelectric material distribution as a technique to improve the energy harvesting efficiency. This work presents some results on the topological optimization of the piezoelectric layer bonded to a sliding-free plate (base excitation) connected to an electric circuit. This is done using an electromechanical finite element model for laminated piezoelectric plates combined to a genetic algorithm based optimization. The model fully represents the coupling between base structure, piezoelectric layers and circuits. Electric circuit parameters and tip mass value are optimized simultaneously to guarantee best operating conditions for each topology. Additionally, an inductance is considered in parallel with the harvesting circuit impedance as a means to improve the frequency range of the device. Results indicate that topology optimization of the active layers may increase the harvesting efficiency in terms of harvested energy per unit mass of the device. It was also observed that the inclusion of resonant circuits may improve the amount of harvested energy and the effective frequency range of the device.*

Keywords: *Energy harvesting, topology optimization, piezoelectric materials, resonant circuits.*

1. INTRODUCTION

Many modern engineering devices such as microelectromechanical systems, condition monitoring sensors and small mobile electronic gadgets are required to carry their own power supply which normally consists of conventional limited lifespan batteries. The lifespan and performance of such devices could be largely improved if they could harvest, or recycle, ambient or surrounding energy, such as those from the mechanical vibrations of the devices. Over

the last decade, the use of piezoelectric materials as mechanical-to-electrical energy converters for energy harvesting devices has been largely studied [1]. The motivation for the use of such materials in energy harvesting devices is based on their vast employment as distributed sensors and actuators due to their large electromechanical coupling coefficient. Piezoelectric materials can be found in the form of thin layers or patches which can be easily integrated into flexible structures without significant mass increase.

Most of the research found in the open literature explore the use of electromechanical resonant devices tuned to the operational resonance frequency of the host structure or machine in order to maximize the electrical energy harvested or generated. The vast majority of the considered devices is based on a cantilever beam with tip mass with properties that are tuned accordingly so that the device resonance frequency matches the operating frequency. The electrical energy is generated by one or more piezoelectric patches bonded to a cantilever substrate. Through their electrodes, the piezoelectric patches can convert part of their strain energy into usable electrical energy. The induced electric current should be directed to a proper electric circuit responsible for signal rectification and energy storage [2].

The performance of these resonant devices for energy harvesting is greatly dependent on the adequate tuning between resonant and operation frequencies. Any mismatch due to variability of the device properties or operation frequency may lead to large performance losses [3]. Therefore, it is of major importance to well estimate or design the device resonant frequency. Consequently, the predictive model considered to design the device may be extremely important. Although the majority of the studies found in the literature use one degree of freedom models to represent the cantilever beam with tip mass, this simplification may lead to an incorrect prediction of the resonance frequency of the device and, therefore, to an inadequate frequency tuning [4].

On the other hand, few studies have attempted to optimize the geometry of the active piezoelectric layers in order to maximize the energy harvested [5,6,7], although some studies focused on vibration control could be extended to the design of piezoelectric layers for energy harvesting [8,9]. This is, however, not a simple task due to the dependence of energy harvesting performance on the adequate resonance frequency tuning. Any geometrical or topological modification in the piezoelectric layer affects not only the electric output of the device but also its resonance frequency. Hence, a simultaneous optimization, including piezoelectric layer distribution, electric circuit parameters and tip mass, should be used.

This work presents a preliminary study on the optimization of energy harvesting devices based on the standard tip mass cantilever beam but, for which, first a resonant circuit is proposed and then an active layer design methodology is presented. This is done using an electromechanical finite element model for laminated piezoelectric plates combined to a genetic algorithm based optimization. The model fully represents the coupling between base structure, piezoelectric layers and circuits.

2. PROBLEM DESCRIPTION

A piezoelectric energy harvesting device can be designed using a cantilever beam partially covered with piezoelectric layers or patches and a tip mass to adjust the resonance frequency of the device. This was done here using an aluminium plate with dimensions

(60x25x1) mm³ on the surface of which two PZT-5A piezoceramic patches with dimensions (55x25x0.25) mm³ are bonded, as shown in Figure 1. A sliding-free boundary condition is considered for the aluminum plate. A tungsten seismic mass is considered to be attached to the free side of the plate, as shown in Figure 1.

The energy harvesting electric circuit is represented here by a simple electric load with resistance R . The energy dissipated in the electric resistance can be thought then as an upper limit to the potentially harvested energy. To increase the performance of the electric circuit, as an absorber of the structural vibratory energy, an electric inductance L may be connected in series to the resistance.

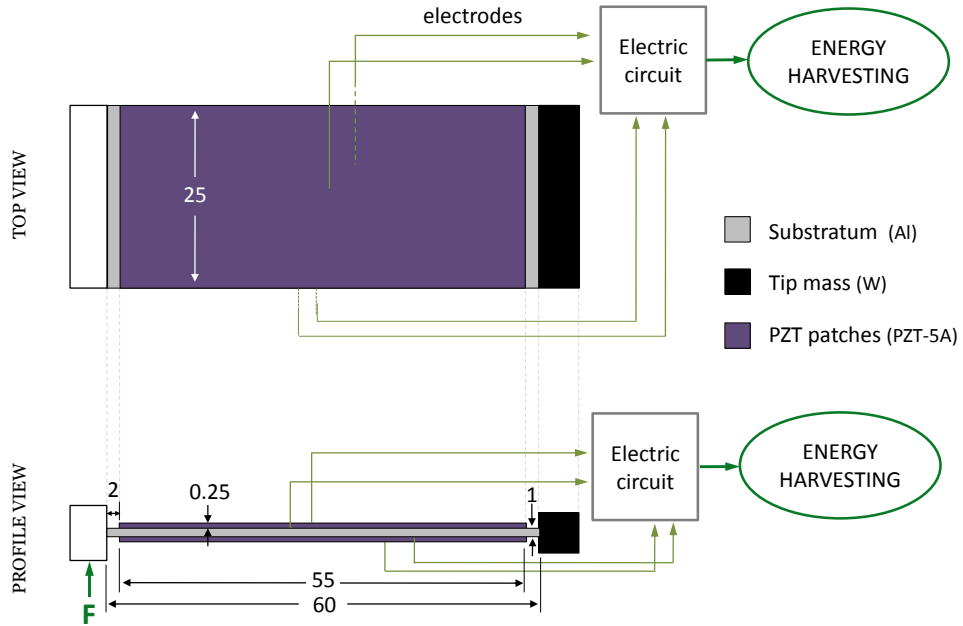


Figure 1. Sliding-free plate with two PZT patches connected to a energy harvesting electric circuit (not in scale, dimensions in mm).

The material properties of the thickness-poled PZT-5A are: $c_{11}^E = c_{22}^E = 96.39$ GPa, $c_{33}^E = 144.91$ GPa, $c_{12}^E = 51.22$ GPa, $c_{13}^E = c_{23}^E = 63.55$ GPa, $c_{44}^E = c_{55}^E = 39.63$ GPa, $c_{66}^E = 22.57$ GPa, $e_{11}^\sigma = e_{22}^\sigma = 15.3$ nFm⁻¹, $e_{33}^\sigma = 15.05$ nFm⁻¹, $\rho^{pzt} = 7750$ kg m⁻³. The aluminium properties are: Young's modulus 70 GPa, Poisson ratio 0.35 and mass density $\rho^{Al} = 2700$ kg m⁻³. For the tungsten tip mass, the mass density is $\rho^W = 15500$ kg m⁻³.

To maximize the energy harvesting performance, it is normally desirable to maximize the strains in the piezoelectric material such that more vibratory energy is available to be converted into electric energy. This can be done by maximizing the vibration amplitude of the cantilever beam for a given excitation. For that, in the case of harmonic excitation of the device, appropriate tuning between the device natural frequency and the operating (excitation) frequency should lead to higher vibration amplitudes. Most common machines vibrate along frequency ranges between 5 and 100 Hz [10]. Based on that, this work considered the operating frequency as 100 Hz.

The seismic mass was implemented in the model considering translational and rotational inertias, at the smaller free end of the plate, which were distributed in the correspondent nodes and, in a similar way a distributed transversal force in the sliding side of the plate was

considered as excitation input. In order to obtain a more practical device design, the tip mass was modeled such that its volume would be minimal and well distributed. Hence, tungsten was chosen due to its high mass density. The tip mass is considered to be a prismatic bar along the plate width with square cross-section, as shown in Figure 1.

The simulations performed in this work used a finite element model for laminated plates with piezoelectric layers connected to electric circuits described in [11]. The model is based on an Equivalent Single Layer (ESL) formulation combined with First-order Shear Deformation Theory for which the layers may have independent electric degrees of freedom. Each piezoelectric layer may be connected to an independent electric circuit with resistance, inductance and voltage source. The connection of circuits and patches considers that the electrodes entirely covers the patches surfaces resulting in an equipotential surface so that the electric charges induced on the piezoelectric layers electrodes are transferred to the electric circuit. The equipotential surface may also be composed of several patches. Considering the equivalence between electric charges in the patches and in the circuits to which they are connected, the following coupled equations of motion can be written [11]

$$\begin{bmatrix} \mathbf{M} & \mathbf{0} \\ \mathbf{0} & \mathbf{L}_c \end{bmatrix} \begin{Bmatrix} \ddot{\mathbf{u}} \\ \ddot{\mathbf{q}}_c \end{Bmatrix} + \begin{bmatrix} \mathbf{0} & \mathbf{0} \\ \mathbf{0} & \mathbf{R}_c \end{bmatrix} \begin{Bmatrix} \dot{\mathbf{u}} \\ \dot{\mathbf{q}}_c \end{Bmatrix} + \begin{bmatrix} \mathbf{K}_m & -\bar{\mathbf{K}}_{me} \\ -\bar{\mathbf{K}}_{me}^t & \bar{\mathbf{K}}_e \end{bmatrix} \begin{Bmatrix} \mathbf{u} \\ \mathbf{q}_c \end{Bmatrix} = \begin{Bmatrix} \mathbf{F}_m \\ \mathbf{V}_c \end{Bmatrix}. \quad (1)$$

The resistance and inductance values were computed using formulas designed to minimize the vibration amplitude of the plate (passive vibration control) at a given frequency, supposing that the energy extracted (dissipated) from the plate could alternatively be stored in a harvesting circuit. In the case of resistive circuit, the loss factor provided to the structure is maximized for the following resistance value [12]

$$R_c = \frac{K_e \sqrt{1 - K_n^2}}{\omega_{OC}^2}, \quad \text{where } K_n^2 = \frac{K_p^2}{K_e \omega_{OC}^2}, \quad (2)$$

where K_e is effective dielectric stiffness of the patches (inverse of their capacitance), K_p is the electromechanical stiffness modal $K_p = \boldsymbol{\phi}^t \bar{\mathbf{K}}_{me}$, that is, a projection of the electromechanical stiffness matrix $\bar{\mathbf{K}}_{me}$ into $\boldsymbol{\phi}$ corresponding to the first bending vibration mode of the device for patches in open-circuit, associated to the resonance frequency ω_{OC} .

In the case of resistive-inductive (resonant) circuit, the vibration amplitude of the structure is minimized using the concept of dynamic vibration absorbers in which the inductance provides an electrical resonance frequency to the circuit that may be tuned to the natural frequency of the structure, so the circuit absorbs the energy from the structure when it vibrates with frequencies close to its natural frequency. The resistance and inductance that maximize the vibration amplitude reduction may be obtained using the formula [11]

$$L_c = \frac{K_e}{\omega_{OC}^2}, \quad R_c = \frac{K_p \sqrt{2K_e}}{\omega_{OC}^2}. \quad (3)$$

An alternative formulation for the design of shunt circuits can be found in [13].

3. PERFORMANCE OF RESISTIVE AND RESONANT HARVESTING DEVICES

In order to evaluate the performance in terms of usable energy harvesting of the device shown in Figure 1, the electromechanical coupled model is used to evaluate the frequency spectrum of the device electric output when subjected to a distributed transversal force located at the sliding side. Two electric circuits were considered, a purely resistive one (R) and a resonant, or resistive-inductive, (RL) one. In both cases, the resistance represents the energy harvesting electric circuit (rectification and storage) such that the energy dissipated by the resistance would be an estimate of the maximum energy that could be harvested.

The design of the device shown in Figure 1 considers that the geometric properties of the aluminium plate with piezoelectric patches remain unchanged, therefore the value of the tip mass was adjusted so that the natural frequency of the device converges to the desired operating frequency (100 Hz).

Since the connection between piezoelectric patches and electric circuit affects the resonance frequency of the device, the tip mass was updated iteratively in conjunction with the design of the electric circuit components (resistance and inductance). In particular, the optimal resistance value for the resistive circuit leads to a decrease in the resonance frequency of the device, as compared to the case of open-circuit piezoelectric patches, but, at the same time, is a function of the open-circuit natural frequency (see Eq. (2)). On the other hand, optimal resistance and inductance values for the resonant circuit replace the original resonance peak by two well-damped coupled resonance peaks with an anti-resonance in between. The anti-resonance frequency is supposed to match the target (operating) frequency. Both resistance and inductance values are functions of the open-circuit natural frequency (see Eq. (3)). Therefore, an iterative procedure was implemented in which the tip mass M_i , and consequently the circuit components, was updated, using $M_{i+1} = (M_i + M_b)(f_i/100) - M_b$, until the peak frequency, for the resistive circuit, or the average between the two peak frequencies, for the resonant circuit, denoted as f_i converged to the target frequency, 100 Hz, within a 2% error margin. M_b is the expected approximate contribution of the plate inertia to the natural frequency of the device and is set to 33/140 of the sum of aluminium plate and piezoelectric patches masses (9.4 g). An initial guess of 90 g was considered for the tip mass based on previous simulations. It was observed that, in general, no more than 3 iterations were necessary. For the resistive circuit, a 89 g tip mass led to a peak frequency at 99.8 Hz, with circuit resistance equal to 13.5 k Ω . For the resonant circuit, a 91 g tip mass led to 99.5 Hz for the average between the two peak frequencies, with circuit resistance and inductance equal to 8.4 k Ω and 22.9 H, respectively. It is worthwhile to notice that this inductance value require a synthetic inductance which will not be discussed here.

The methodology considered for the design of circuit components focuses on reducing the vibration amplitude of the structure, therefore it is convenient to analyze the frequency response of the structure represented by the transversal velocity at the sliding side per unit transversal force applied at the same location (Figure 2). As shown in Figure 2, the RL circuit is much more effective in reducing the vibration amplitude of the structure. In fact, it is known that the resistive (R) circuit acts as a viscoelastic damper with relatively small loss factor, while the resonant (RL) circuit acts as a dynamic vibration absorber, which absorbs the vibratory energy of the structure around the circuit natural frequency and then dissipate

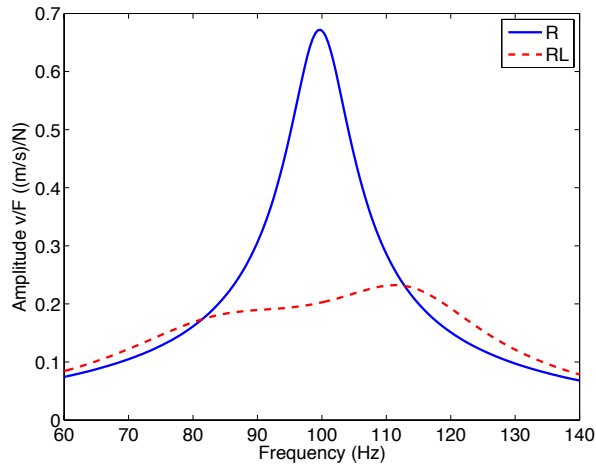


Figure 2. Frequency response amplitude of velocity per unit force at the sliding side.

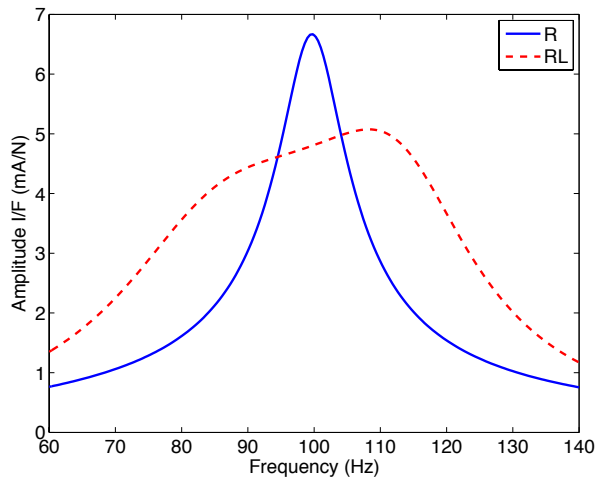


Figure 3. Frequency response amplitude of electric current at harvesting circuit per unit force.

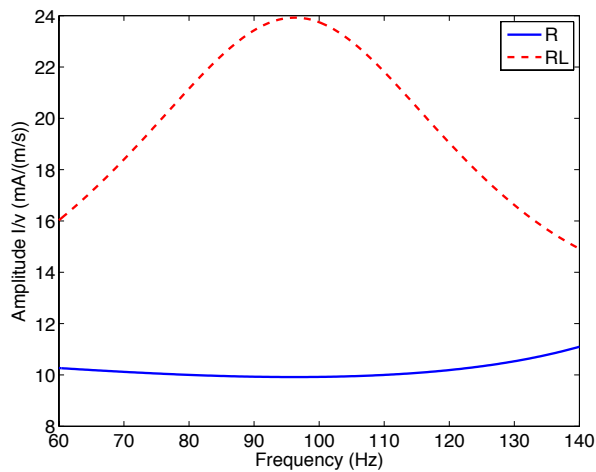


Figure 4. Frequency response amplitude of electric current at harvesting circuit per unit velocity at the sliding side.

it through the resistance [11]. Thus, it is suggested here that this vibratory energy, dissipated

by the electrical resistance, could be stored if the resistance was to be replaced by a proper harvesting circuit. In this case, the RL circuit is promising compared to the R circuit, since it is considerably more effective in extracting energy from the structure.

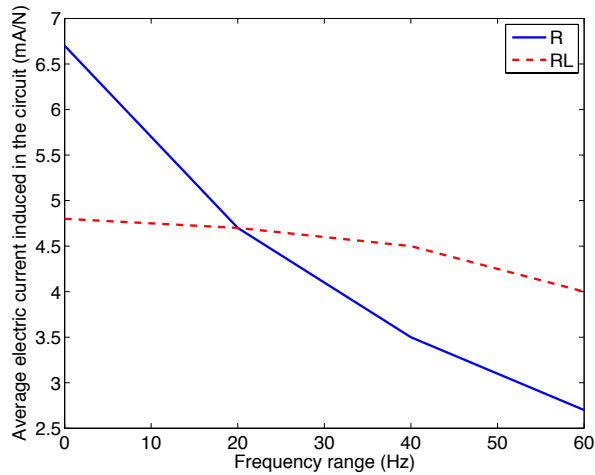


Figure 5. Average electric current per unit force for different frequency ranges.

Figure 3 shows the frequency response of the device, when excited by the transversal force and observed by the electric current induced in the circuit. It may be noticed that the RL circuit could be more interesting if there was an uncertainty in the input frequency since it flattens the peak response and, thus, leads to a wider effective frequency range. However, at the target frequency or within a narrow frequency range around the target frequency, the resistive circuit leads to higher electric output. By increasing the frequency range, around the operating frequency, it was observed that the average induced electric current becomes considerably larger for the resonant circuit, while the one for the circuit R decreases rapidly (Figure 5).

The above analysis indicates that for a given excitation, the energy potentially harvested by the resistive circuit can still be higher than the one of the resonant circuit, even if only in a very narrow frequency range. However, Figure 2 shows that for the same excitation, the vibration amplitude of the device is bigger for the resistive circuit (as it is less efficient in dissipating vibratory energy). This indicates that in Figure 3, the input power could be different in the cases of resistive and resonant circuit. Therefore, an alternative analysis of energy harvesting could be performed using the induced electric current per unit velocity at the sliding side. It is suggested here that this measure represents better the efficiency of the device to convert motion into electric current and, on the other hand, could be a better measure of efficiency in energy conversion. Thus, Figure 4 shows the frequency response amplitude of induced electric current per unit velocity at the sliding side. Note that, in this case, the induced electric current is always superior for the resonant circuit.

4. GEOMETRIC OPTIMIZATION OF PIEZOELECTRIC PATCHES

From the previous analysis, it is clear that proper tuning of device natural frequency and electric circuit parameters may improve the potentially harvested electric energy. However, the amount of electric current induced in the piezoelectric patches depends not only on

their effectiveness in converting strain energy into electric charge but also on how much vibration amplitude, and thus strain energy, the device experiences. Therefore, the stiffness and inertia added by the piezoelectric patches to the substrate should also play a role in the energy harvesting operation.

Then, it is reasonable to expect that the geometry of the piezoelectric patches could be optimized in order to maximize the corresponding energy harvested. Hence, this section presents a methodology for improving the energy harvesting performance of a device by shaping the piezoelectric patches.

4.1. Optimization strategy

The procedure to optimize the shape of the piezoelectric patches consists on optimizing the distribution of a fixed number of piezoelectric patches over the upper and lower surfaces of a host metallic plate (substrate). Starting from the device studied previously, the upper and lower piezoelectric patches are divided into a 55 smaller patches (Figure 6). It is then desired to select 30 of them that maximize the electric current induced in the circuit.

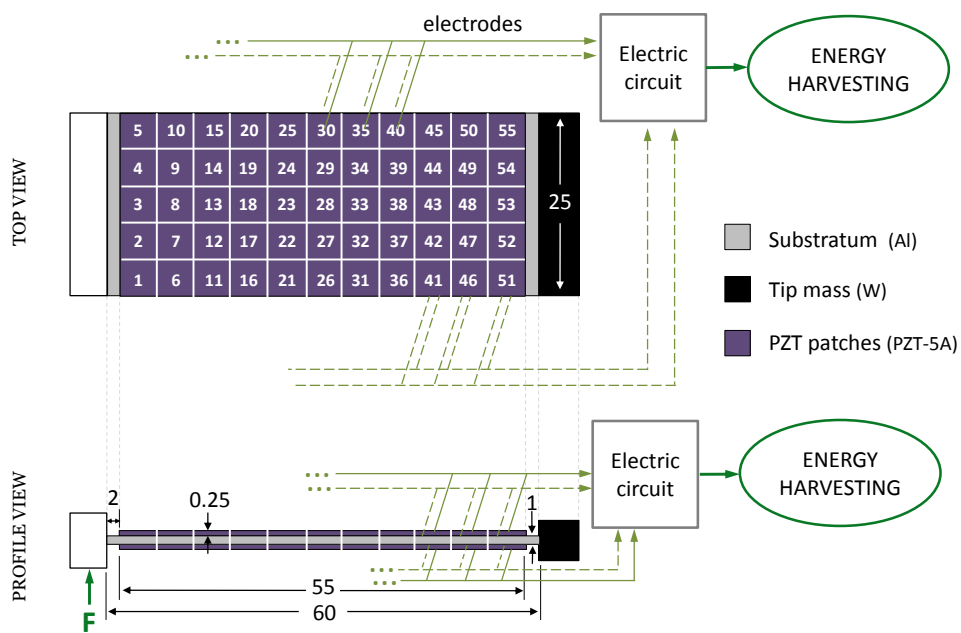


Figure 6. Possible locations for the 30 selected piezoelectric patches over the substratum.

This is done using a topological approach i.e., several configurations (topologies) of 30 piezoelectric patches located in 30 of the 55 possible locations are tested and their energy harvesting performance are evaluated. Although there could be some indications of interesting piezoelectric patches shapes by using concepts of modal strain energy distribution and shaped (distributed) modal sensors, some preliminary numerical simulations have shown that some logical (expected) topologies may be good but not optimal. This seems to be mostly due to the fact that the presence of the piezoelectric patches affects significantly bending stiffness and mass distribution of the multilayer structure.

Therefore, an automatic optimization strategy is needed to explore the research space in an efficient manner. An extensive search of the possible combinations of 30 locations from the 55 available would lead to an impracticable computational cost, since more than 10^{15} ($C_{55,30}$) combinations would have to be evaluated. Genetic Algorithms, GAs, are more suitable search methods in these cases when the research space is too large, strongly multimodal and non-linear. It is chosen here to setup a GA search by defining a random initial population formed by so-called individuals with chromosomes that are composed of 30 genes as illustrated in Figure 7. Each gene is an integer number from 1 to 55 representing the location index. Therefore, one individual represents a topology formed by 30 patches with location defined by its genes.

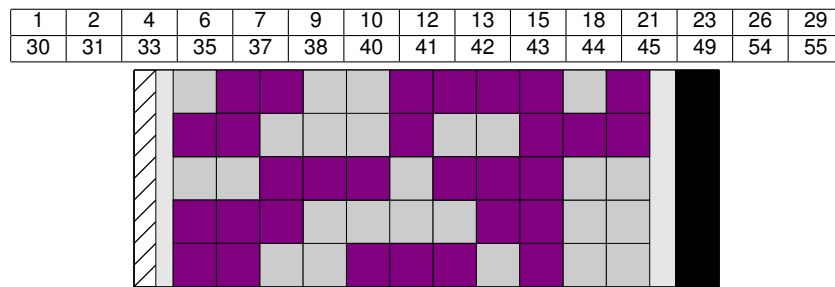


Figure 7. Arbitrary representation of a topology candidate containing 30 patches.

Following the standard GA evolution process, the initial population is considered to evolve along a set of generations through reproduction (crossover), mutation and selection operations. While reproduction and mutation operations aim to provide diversity to the population, the selection operation aims to rank individuals with respect to a fitness or objective function. Since this is a random search algorithm, the optimal results are dependent on the initial population and on the reproduction, mutation and selection parameters. However, it is expected that for a sufficiently large number of generations or size of the initial population, the algorithm will converge to the global optimum.

Since any individual of the population is composed by 30 different integer numbers in the domain $[1, \dots, 55]$, a specific routine was written to build the initial population. For each individual, the routine scrambles randomly a vector of integers from 1 to 55 and, then, the first 30 elements of the scrambled vector define the corresponding individual. This procedure is repeated for all individuals in the initial population. The selection of the first 30 elements in the scrambled vector does not imply a tendency since the distribution of the sensor indices in the vector is equiprobable.

The mutation operation, considered in this work, consists in replacing one of the 30 genes (patch locations), selected randomly, of an individual by another one, selected randomly from the complementary group of patch locations, that is, from the 25 remaining patch locations not present in the individual. This procedure prevents the generation of an individual with repeated genes. The reproduction (crossover) operation consists of an arithmetic mean of two individuals (parents) to form a new individual (child), where the rounding between two integer genes is performed randomly. In this case, the generation of an individual with repeated genes is possible and, when this is the case, the fitness function of this individual is not evaluated to save computational time; instead a small fitness value is attributed to it, such

that its selection probability is also small. The selection operation is based on a stochastic universal sampling algorithm, where the expectation of individuals in the population is evaluated from a fitness ranking.

Besides the choice of reproduction, mutation and selection operators, it is necessary to define the size of the initial population (N), the number of best individuals (elite) which are kept unmodified from one generation to another (Σ), the percentage of the population in each generation which are generated by crossover (T_c) and the total number of generations the population evolves (N_p). Once defined T_c , the remaining part of population is generated by either the previous elite or mutation operation.

Apart from the procedures proposed for the construction of the initial populations, the mutation and reproduction operations and the parameters' definition, the optimization was performed using operators and algorithms of MATLAB Genetic Algorithm and Direct Search (GADS) Toolbox.

4.2. Objective function to rank harvesting performance

The objective of the present optimization is to find the topology of an array with 30 piezoelectric patches that maximizes the average electric current output, over a narrow frequency range (20 Hz) around a target frequency (100 Hz), for a given fixed force excitation. The topology directly affects the effective electromechanical modal stiffness K_p and the effective bending stiffness. Therefore, for each individual (topology) the following procedure is performed:

1. First, the natural frequencies and vibration modes are computed for open-circuit condition in order to obtain a first approximation of the effective modal electromechanical stiffness K_p , the squared modal electromechanical coupling coefficient K_n^2 and the optimal circuit resistance R ;
2. Then, the (damped) natural frequency for the device connected to the resistive circuit is computed to qualify the resonance frequency tuning and adjust the tip mass accordingly, using $M_{i+1} = (M_i + M_b)(f_i/100) - M_b$;
3. With the new tip mass, the natural frequencies and vibration modes are computed again to obtain the effective modal electromechanical stiffness K_p , the squared modal electromechanical coupling coefficient K_n^2 and the optimal circuit resistance R_{i+1} ;
4. If the frequency f_i has converged to the target frequency or 3 iterations were performed, the frequency response function of electric current induced in the circuit per unit velocity at the sliding side, is evaluated using the coupled equations of motion and its 20 Hz frequency range average is computed using $\bar{G}_{Iv} = (1/\Delta\omega) \int G_{Iv} d\omega$.

In most cases with one or two iterations, satisfactory tuning between resonance and target frequency was observed.

5. OPTIMIZATION RESULTS

This section presents preliminary results obtained from the optimization of piezoelectric patches topologies. The following parameters were set for the GA optimization: initial population of $N = 1000$ individuals, crossover rate at $T_c = 30\%$, elite population of $\Sigma = 5$ individuals and termination criteria at $N_p = 15$ generations.

The optimal topology is represented schematically in Figure 8 and the average electric current induced in the circuit for different frequency ranges may be observed in Figure 11. Using this topology, the peak induced electric current at the target frequency of 100 Hz is 5.7 mA/N for the R circuit and 4.7 mA/N for the RL circuit. This performance can be compared to the one of the full piezoelectric patch (55x25 mm) presented previously (6.7 mA/N and 4.8 mA/N, respectively). This means that 85% of original electric current is obtained with a little more than half (55 %) the piezoelectric material volume, for the resistive circuit, and 98%, to the resonant circuit.

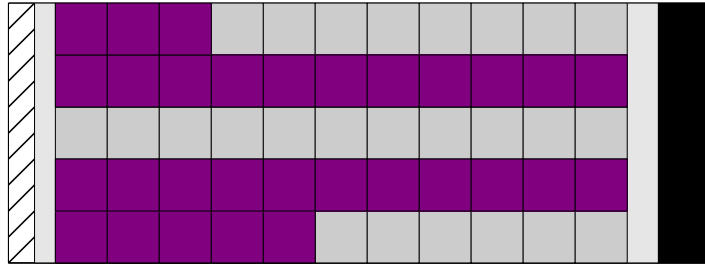


Figure 8. Optimal topology leading to the maximum electric current output of 3.1 mA/N or 5.4 mA/(m/s).

The average induced electric current in a 20 Hz wide frequency range around the target frequency of 100 Hz is 3.1 mA/N for the R circuit and 4.6 mA/N for the RL circuit, compared to those provided by the 55x25 mm patch (4.8 mA/N and 4.8 mA/N, respectively). In this case, 65% of original electric current is obtained with a little more than half (55 %) the piezoelectric material volume for the resistive circuit and 96% for the resonant circuit.

The reduction of device total mass is not the same as the reduction of piezoelectric material volume since the optimal topology leads to a little increase in the tip mass, from 89 g to 93 g for the resistive circuit and from 91 g to 92 g for the resonant one. Therefore, the device total mass for the resistive circuit is reduced by 9.2%, from 102.4 g to 93.8 g, and by 3% for the resonant circuit, from 101.4 g to 98 g.

The optimal resistance of the resistive circuit for the optimal topology was found to be $\sim 26 \text{ k}\Omega$ compared to $\sim 13 \text{ k}\Omega$ for the original full patch. Considering a simple approximation for the expected average power output $P_a = RI_a^2$, the optimal topology combined to a resistive circuit would provide a power output of 604 mW/N, that is 72% of the one corresponding to the full patch 844 mW/N.

Figures 9 and 10 show the frequency response amplitude of electric current per unit force and per unit velocity, respectively. It can be noticed that the general behavior is very similar to the one obtained for the full patch. However, the performance of the resistive circuit is more sensitive to the decrease of piezoelectric material than the resonant circuit. This can

also be observed from Figure 11, where the resonant circuit starts outperforming the resistive one from a narrower frequency range (~ 10 Hz), as compared to the previous case of the full piezoelectric patch (~ 20 Hz).

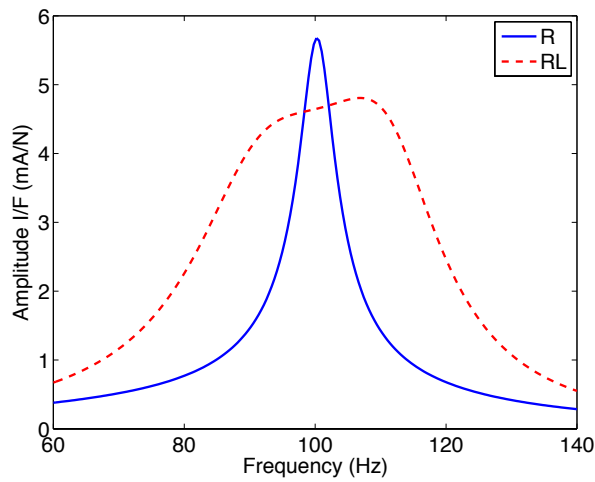


Figure 9. Frequency response amplitude of electric current at harvesting circuit per unit force for the optimal topology.

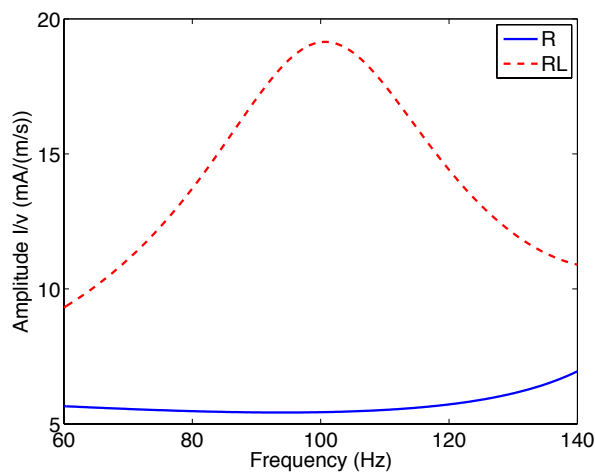


Figure 10. Frequency response amplitude of electric current at harvesting circuit per unit velocity at the sliding side for the optimal topology.

The asymmetry of the optimal topology could be undesired, since a symmetric topology could be more straightforward to design and manufacture. For this reason, a symmetrized topology derived from the optimal topology was tested and is shown in Figure 12. It was observed that the symmetric design (Figure 12) leads to almost the same performance of the optimal design.

6. CONCLUSIONS

This work presented an analysis of a resonant piezoelectric energy harvesting device focusing on the improvement of the system performance through the inclusion of a resonant

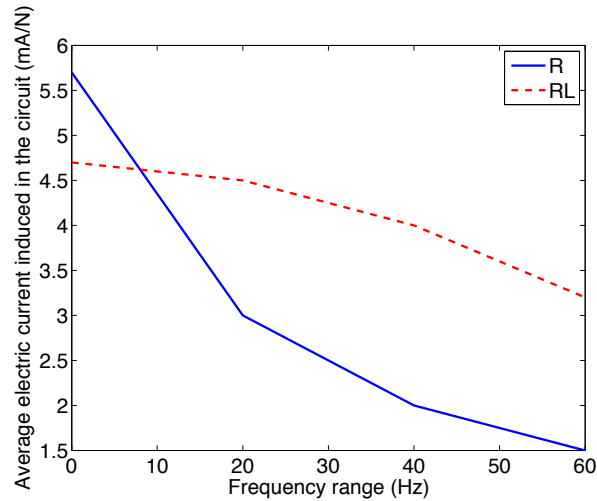


Figure 11. Average electric current per unit force induced in the circuit for different frequency ranges to optimal topology with 30 piezoelectric patches.

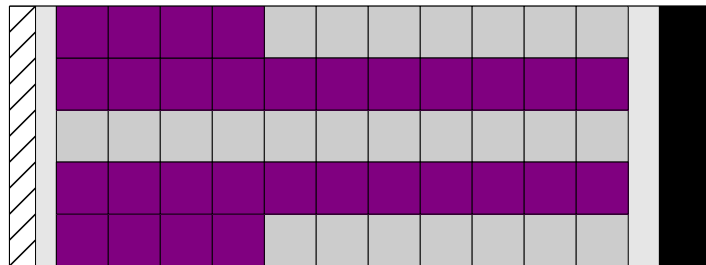


Figure 12. Symmetrized optimal topology. Electric current output 3.0 mA/N or 5.4 mA/(m/s).

electric circuit and on the geometric optimization of the piezoelectric active layer. Results indicate that the inclusion of resonant circuits is promising since it may lead to effective energy harvesting over a wider frequency range and a performance more robust to frequency uncertainties. As for the geometric optimization of the active layer, results indicate that more cost-effective devices may be obtained but optimal topologies are not straightforward.

Acknowledgments

The authors acknowledge the financial support of MCT/CNPq/FAPEMIG National Institute of Science and Technology on Smart Structures in Engineering, grant 574001/2008-5, and CAPES/COFECUB Program, grant Ph 672/10.

7. REFERENCES

- [1] Sodano H.A., Inman D.J. and Park G., "A review of power harvesting from vibration using piezoelectric materials". *Shock and Vibration Digest*. 36(3):197-206, 2004.
- [2] Guan M.J. and Liao W.H., "On the efficiencies of piezoelectric energy harvesting circuits towards storage device voltages". *Smart Materials and Structures*. 16(2):498-505, 2007.
- [3] Adhikari S., Friswell M.I. and Inman D.J., "Piezoelectric energy harvesting from broadband random vibrations". *Smart Materials and Structures*. 18(11):115005, 2009.
- [4] Erturk A. and Inman D.J., "Issues in mathematical modeling of piezoelectric energy harvesters". *Smart Materials and Structures*. 17:065016, 2008.
- [5] Friswell M.I. and Adhikari S., "Sensor shape design for piezoelectric cantilever beams to harvest vibration energy". *Journal of Applied Physics*. 108(1):014901, 2010.
- [6] Nakasone P.H. and Silva E.C.N., "Design of piezoelectric energy harvesting devices and laminate structures by applying topology optimization". *Proceedings of 16th SPIE Annual International Symposium Smart Structures and Materials and Nondestructive Evaluation and Health Monitoring*. 7286, 2009.
- [7] Rupp C.J., Evgrafov A., Maute K. and Dunn M.L., "Design of piezoelectric energy harvesting systems: A topology optimization approach based on multilayer plates and shells". *Journal of Intelligent Material Systems and Structures*. 20(16):1923-1939, 2009.
- [8] Vasques C.M.A. and Rodrigues J.D., "Passive vibration control with shunted modal piezoelectric transducers". *Proceedings of the IV ECCOMAS Thematic Conference on Smart Structures and Materials*. A. Cunha et al., eds., Porto, Portugal, 2009.
- [9] Pagani Jr. C.C. and Trindade M.A., "Optimization of modal filters based on arrays of piezoelectric sensors". *Smart Materials and Structures*. 18(095046), 2009.
- [10] Priya S., Inman D.J., "Energy harvesting Technologies". Ed.1, *Springer*, 2009.
- [11] Godoy T.C. and Trindade M.A., "Modeling and analysis of laminate composite plates with embedded active-passive piezoelectric networks". *Journal of Sound and Vibration*. 330:194-216, 2011.
- [12] Trindade M.A. and Maio C.E.B., "Multimodal passive vibration control of sandwich beams with shunted shear piezoelectric materials". *Smart Materials and Structures*. 17:055015, 2008.
- [13] Thomas O., Deü J.-F. and Ducarne J., "Vibrations of an elastic structure with shunted piezoelectric patches: efficient finite element formulation and electromechanical coupling coefficients". *International Journal for Numerical Methods in Engineering*. 80(2):235-268, 2009.